

## IMPROVED DUAL BAND-NOTCHED UWB SLOT ANTENNA WITH CONTROLLABLE NOTCHED BANDWIDTHS

C. M. Li and L. H. Ye

School of Electric Power  
South China University of Technology, Guangzhou 510640, China

**Abstract**—A compact dual band-notched ultra-wideband slot antenna with sharp band-notched characteristics and controllable notched bandwidths is presented. The antenna is formed by a rectangular slot with chamfered corners on a printed circuit board ground plane, a T-shaped stub and two sets of compound band-notched structures. The compound band-notched structures are employed to generate desired lower and upper rejected bands with satisfactory skirt characteristics and sufficient rejection bandwidths. Moreover, the bandwidth of either the lower or upper rejected band can be independently adjusted by changing the size and location of the corresponding band-notched structure. Finally, a UWB slot antenna with two rejected bands at WiMAX/WLAN frequencies is successfully simulated, designed, and measured, showing good impedance matching, stable gain and near omnidirectional radiation patterns.

### 1. INTRODUCTION

Ultra-wideband antennas have attracted great attention in the recent years [1–6]. However, over the designated UWB frequency range, there are existing narrow bands used by worldwide interoperability for microwave access (WiMAX) operation in the 3.3–3.7 GHz band and wireless local area network (WLAN) in the 5.15–5.825 GHz band. Therefore, it is desired to design the UWB antenna with dual-notched bands in 3.3–3.7 GHz and 5–6 GHz to minimize the potential interference. Recently, a number of UWB antennas with band-notched

characteristics have been discussed [7–14] and various methods have been used to achieve band notched function, such as embedding a slot of different shapes in the radiating patch [7–10], using parasitic patches [11, 12], embedding a slit in the feeding strip [13], or etching split ring resonator (SRR) coupled to the feed-line [14]. However, each approach above only creates one single filtering frequency and is not able to provide satisfactory skirt characteristics and a sufficient rejection bandwidth. In addition, all of the antennas mentioned above have concerned no more than two notched bands and most of them only have one notched band, which can not fulfill dual or multi-rejected band function. A few dual or multi-rejected band UWB antennas were presented [15, 16]. However, the band-notched characteristics of these antennas are not desirable to avoid the interference problem within the UWB operating band. Obtaining high effective band-notched characteristics is a challenging issue. The main problem of the band rejected function design is the difficulty of controlling bandwidth of the notched band, and few band-notched UWB antennas with controllable rejected bandwidth have been presented.

A compact slot UWB antenna with two improved notched bands is proposed. The dual band-notched operation is achieved by embedding two sets of composited band-rejected structures on the rectangular slot with chamfered corners or the T-shaped stub. The desired frequency notched bands can be easily achieved by adjusting the total lengths of the rejected structures. Moreover, by changing the sizes and locations of the compound band-rejected structures, the rejected bandwidths can be effectively controlled. The geometries and design guidelines of single band-notched slot UWB antennas are first introduced in Section 2, while the two improved band-notched UWB antenna is demonstrated in Section 3.

## 2. SINGLE BAND-NOTCH UWB ANTENNA DESIGNS

### 2.1. UWB Antenna Design

Figure 1 shows the geometry of the proposed UWB antenna printed on a 0.8 mm thick substrate with relative permittivity 2.55. A rectangular slot with chamfered corners is fed by a  $50\ \Omega$  coplanar waveguide (CPW) transmission line. The electromagnetic simulation software Ansoft HFSS v11 is employed to perform this design, and good impedance matching over a broad frequency range can be obtained. As shown in Figure 2, the measured bandwidth of the antenna is from 2.9 GHz to more than 11 GHz.

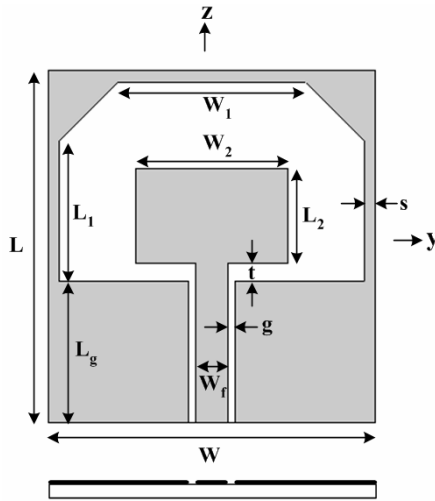


Figure 1. Geometry of the UWB antenna.

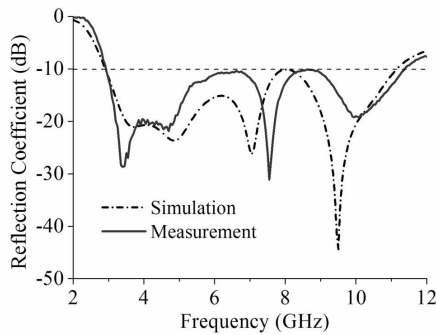
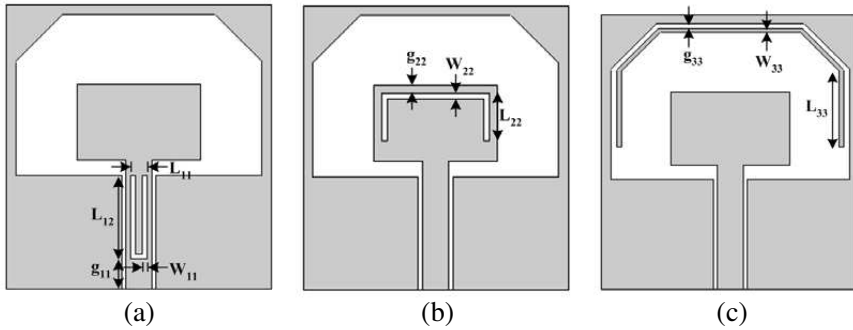


Figure 2. Simulated and measured reflection coefficient of the UWB antenna.

### 2.2. Single Band-notched UWB Antenna Design

In order to reduce the interference from the existing narrow communication systems, the band-notched function is desirable in the UWB system. Three types of band-rejected UWB slot antennas are presented, and their geometries are shown in Figure 3. The first type of the band-notched slot UWB antenna embedded a C-shaped slit in the feeding line is presented in Figure 3(a) (referred to as antenna 1 in this paper). The second design etches an inverted C-shaped slit on the top side of the T-stub, as shown in Figure 3(b) (denoted as



**Figure 3.** Geometries of three band-rejected designs embedding. (a) A C-shaped slit in the feed line, (b) an inverted C-shaped slit in the T-stub, and (c) a parasitic strip in the aperture.

antenna 2). The third band-rejected UWB antenna embedded an inverted C-shaped strip near the top edge of the aperture is depicted in Figure 3(c) (referred to as antenna 3). In these designs, each band-rejected structure of the embedding parasitic slits or strip is able to provide a single filtering frequency in a certain band and functions as a first order stop filter. By properly changing the total lengths of the slits and strip, the desired rejected band frequencies can be easily obtained. Furthermore, the filter resonator of strip or slit embedded on the antenna is much more sensitive to retune due to nearby objects compared to an external filter component. The effects of fixed components nearby the filter have been considered in our design.

It is necessary to control the notched bandwidth to obtain an effective band-notched UWB antenna. Therefore, the rejected bandwidths via the widths and positions of the band-notched structures are investigated. The specific frequency around 5.5 GHz for comparing the effects on the widths and positions of these parasitic slits and strip is selected. Since the rejected frequency shifts a lot corresponding to the length of the slit or strip, the effects of the length of the slit or strip cannot be compared here. Figure 4 exhibits the comparison of the notched bandwidth via the width  $L_{11}$  of the slit embedded in the feed-line for antenna 1. The narrow width  $L_{11}$  of the slit has a narrow notched band, while the wide width  $L_{11}$  has wide band-notched characteristics. The results clearly indicate that the notched bandwidth of the antenna 1 can be effectively controlled by adjusting the width  $L_{11}$  of the parasitic slit.

The band-notched characteristics for antenna 2 based on the location and width of the parasitic slit on the T-stub is studied.

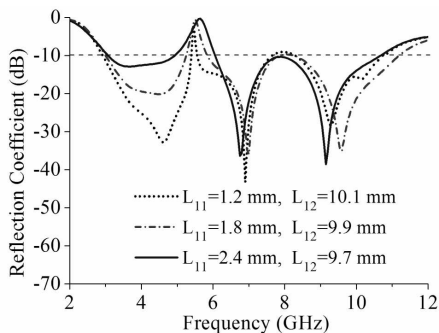


**Figure 4.** Effects of the width  $L_{11}$  and length  $L_{12}$  of the embedding slit on the notched bandwidth for antenna 1;  $g_{11} = 7$  mm,  $W_{11} = 0.3$  mm.

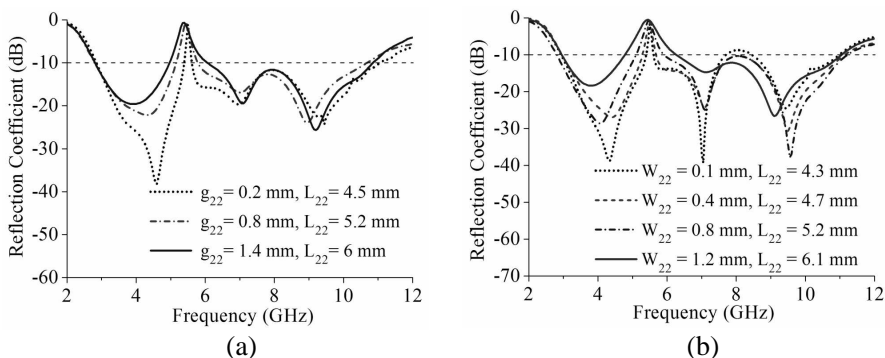


**Figure 5.** Effects of parameters. (a)  $g_{22}$ ,  $L_{22}$ , (b)  $W_{22}$ ,  $L_{22}$  of the embedding slit on the notched bandwidth for antenna 2.

Figure 5(a) shows the effects of the location  $g_{22}$  of the parasitic slit on the notched bandwidth. In this case, the width  $W_{22}$  of the slit is fixed to be 0.3 mm, and large effects on the band-notched function are seen. Results show that the notched bandwidth for antenna 2 becomes wider when  $g_{22}$  increases from 0.2 to 1.4 mm. Figure 5(b) shows the simulated reflection coefficient as a function of  $W_{22}$ , the width of the slit, and the results for the width  $W_{22}$  varied from 0.1 mm to 1.2 mm are presented. In this case, the location  $g_{22}$  of the slit is selected to be 0.5 mm. It is observed that narrow width  $W_{22}$  generates narrow notched bandwidth, while the wide width  $W_{22}$  has a wide notched bandwidth. These results indicate that the location  $g_{22}$  and width  $W_{22}$  of the parasitic slit are important to control the rejected bandwidth for antenna 2.

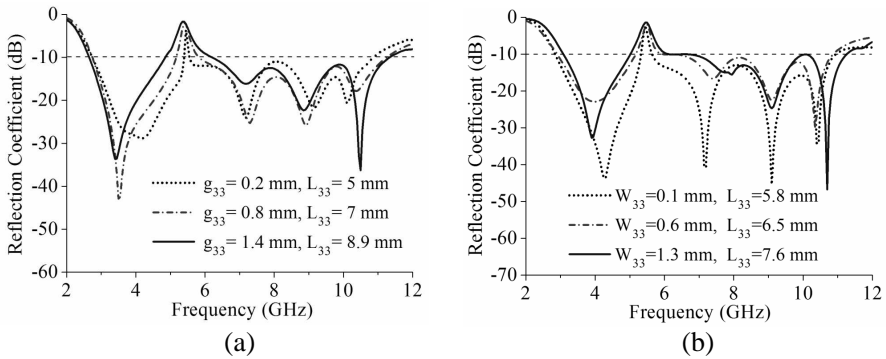


**Figure 6.** Effects of parameters (a)  $g_{33}$ , (b)  $W_{33}$  of the parasitic strip on the rejected bandwidth for antenna 3.

The rejected bandwidth of antenna 3 for location  $g_{33}$  and width  $W_{33}$  of the parasitic strip is also analyzed. Figure 6(a) presents the simulated reflection coefficient for the location  $g_{33}$  varied from 0.2 to 1.4 mm. In this case, the width  $W_{33}$  is fixed to be 0.5 mm. A larger value of  $g_{33}$  generates a wider rejected bandwidth. The notched bandwidth for the width  $W_{33}$  of the parasitic strip is shown in Figure 6(b). In this condition, the location  $g_{33}$  of the strip is selected to be 0.8 mm, and noteworthy effects on the band-notched characteristics are seen. The notched bandwidth is enhanced as  $W_{33}$  increases from 0.1 to 1.3 mm. These results clearly demonstrate that the notched bandwidth of the antenna 3 can be effectively adjusted by changing the position  $g_{33}$  and width  $W_{33}$  of the embedding strip.

### 2.3. Improved Single Band-notched UWB Antenna Design

Three band-notched UWB slot antennas have been described to reduce the interference from the existing narrow communication systems. However, each of the band-notched structures only creates one single filtering frequency within the UWB band and cannot be able to provide satisfactory skirt characteristics and a sufficient rejection bandwidth, which cannot effectively minimize the potential interference with existing narrow bands. In order to achieve a certain notched band with satisfactory skirt characteristics and a sufficient rejection bandwidth, two sets of compound band-notched structures added to the UWB antenna shown in Figure 1 are presented. The first type of the UWB slot antenna with composite band-notched structure formed by a C-shaped slit embedded in the feed-line and an inverted C-shaped slit near the top edge of the T-stub is shown in Figure 7(a) (referred to

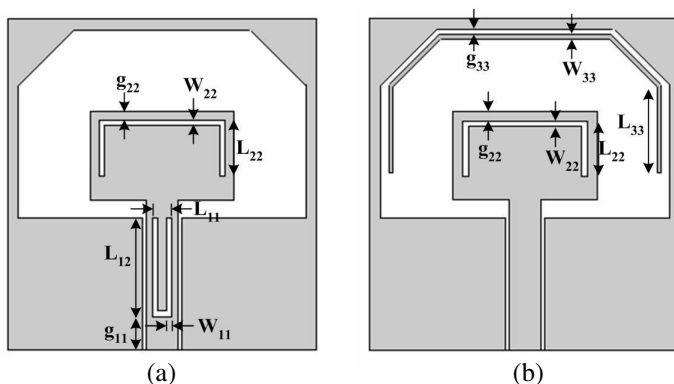


**Figure 7.** Geometries of two band-rejected UWB antennas with composite band-notched structure; (a) embedding a C-shaped in the feed line and a C-shaped slit on the T-stub, and (b) etching a C-shaped in the T-stub, and a parasitic strip in the aperture.

as antenna 4), while the second antenna with compound band-rejected structure consisted of an inverted C-shaped slit near the top edge of the T-stub and an inverted C-shaped strip near the top edge of the near-rectangular aperture is shown in Figure 7(b) (referred to as antenna 5). As discussed above, the embedding slits or strip would generate a single filtering frequency in the UWB operating band and functions as a first order filter. So in these designs, each composite band-rejected structure is able to create two filtering frequency points in a certain band. When these two filtering frequencies are coupled together, an improved notch-band with sharp characteristics can be obtained. In this way, each set of composite band-notched structures functions as a second order filter. The design rules of the integrated band-notched structures are similar to that of a second order stop filter. However, the resonant elements of the integrated band-notched structures are not placed nearby the transmission line regularly like a standard stop filter, so it is difficult to compare the integrated filter with a standard filter. Our further work is to establish equivalent relationship between the compound filter and a standard filter.

Figure 8 illustrates the comparison of band-notched characteristics via different lengths of the embedding slits for antenna 4. In the picture,  $L_{\text{slit1}}$  denotes the overall length of the C-shaped slit embedded in the feed-line while  $L_{\text{slit2}}$  represents the total length of the inverted C-shaped slit near the top edge of the T-stub. Two separate filtering frequency bands are achieved when the total lengths of the slits differ much. When the total lengths of these slits differ slightly, two filtering

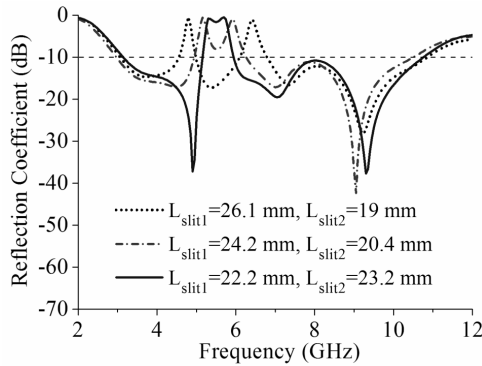


**Figure 8.** Band-notched characteristics with different lengths of the parasitic slits for antenna 4;  $g_{11} = 7$  mm,  $W_{11} = 0.5$  mm,  $L_{11} = 2$  mm,  $g_{22} = 0.5$  mm,  $W_{22} = 0.5$  mm.

frequencies are coupled together to shape a much sharper, wider, and deeper notched band.

As discussed above (seen from Figures 4, 5, 6), the design parameters  $L_{11}$  of the slit embedded in the feed-line,  $g_{22}$  and  $W_{22}$  of the slit on the T-stub,  $g_{33}$  and  $W_{33}$  of the parasitic strip have large effects on the notched bandwidth for antennas 1, 2 and 3, respectively. Since the compound band-notched structures are formed by the embedding slits and strip, the effects of the widths and locations of the slits and strip on the band-notched bandwidth need to be analyzed. Figure 9(a) shows the effects of the width  $L_{11}$  and the location  $g_{22}$  on the notched bandwidth for antenna 4. In this case, the parameter  $W_{22}$  is fixed to be 0.3 mm. The narrow  $L_{11}$  and  $g_{22}$  has a narrow notch bandwidth, while the wide  $L_{11}$  and  $g_{22}$  has a wide rejection bandwidth. Figure 9(b) presents the effects of the parameters  $L_{11}$  and  $W_{22}$  on the band-notched characteristics. In this case, the parameter  $g_{22}$  is selected to be 0.6 mm. It is observed that the rejected bandwidth is obviously enhanced as  $L_{11}$  and  $W_{22}$  increase. From discussion in Figures 4 and 5, the filtering bandwidth becomes wider as  $L_{11}$ ,  $W_{22}$  or  $g_{22}$  increase. For antenna 4, both the filtering bands generated by the slits of the composite structures become wider as the parameters  $L_{11}$ ,  $g_{22}$  and  $W_{22}$  of the band-notched structures increase, which are coupled together to shape a wider notched band. This analysis clearly indicates that the notched bandwidth of the antenna 4 can be effectively controlled by adjusting the values of  $L_{11}$ ,  $g_{22}$  and  $W_{22}$  of the parasitic slits.

The band-notched bandwidth based on the locations and widths of the parasitic slit and strip for antenna 5 is also studied. The effects

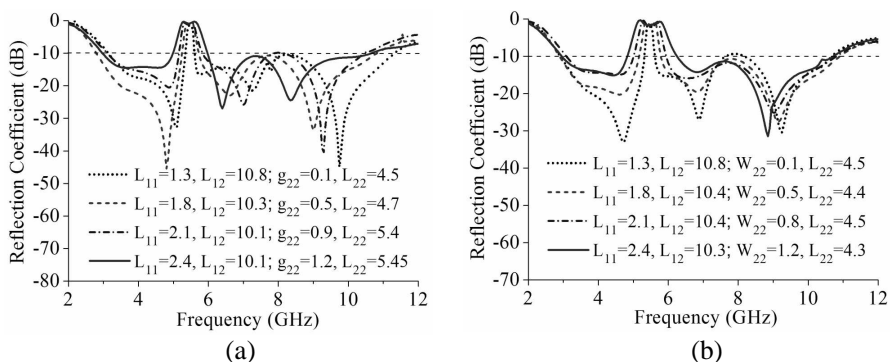


**Figure 9.** Effects of parameters  $L_{11}$ ,  $g_{22}$ , and  $W_{22}$  on the rejected bandwidth for antenna 4 (units: mm).

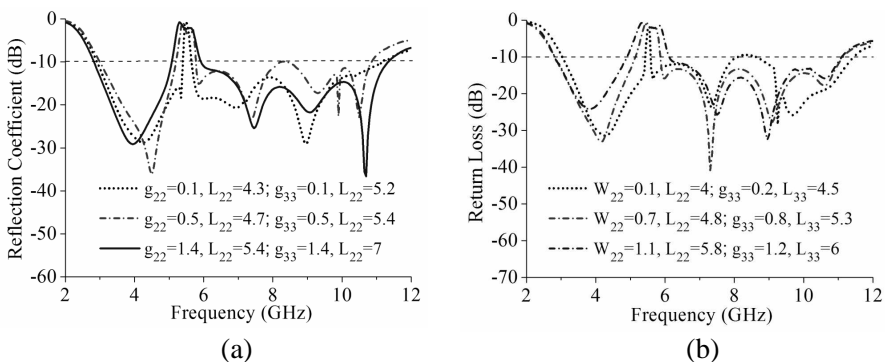


**Figure 10.** Effects of parameters  $g_{22}$ ,  $W_{22}$  and  $g_{33}$  on the rejected bandwidth for antenna 5 (units: mm);  $W_{33} = 0.4$  mm.

of the parameters  $g_{22}$  and  $g_{33}$  on the band-notched bandwidth are studied in Figure 10(a), in which the width  $W_{22}$  of the slit is fixed to be 0.4 mm. Results show that the filtering bandwidth becomes wider as  $g_{22}$  and  $g_{33}$  increase from 0.1 to 1.4 mm. Figure 10(b) shows the simulated reflection coefficient as a function of  $W_{22}$  and  $g_{33}$ . In this case, the location  $g_{22}$  of the slit is selected to be 0.6 mm. It is observed that small values of  $W_{22}$  and  $g_{33}$  generate a narrow notched bandwidth, while large  $W_{22}$  and  $g_{33}$  generate a wide notched bandwidth. This analysis indicates that the location  $g_{22}$ ,  $g_{33}$  and width  $W_{22}$  of the band-rejected structure are important to control the rejected bandwidth for antenna 5.

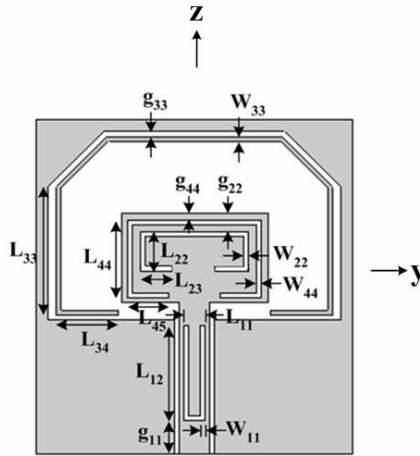


**Figure 11.** Geometry of the proposed dual band-notched slot UWB antenna.

### 3. TWO IMPROVED NOTCHED BANDS UWB ANTENNA

Besides WLAN systems, WiMAX from 3.3–3.7 GHz also operates in the UWB band. To minimize the potential interferences between UWB system and narrowband systems, a dual band-notched UWB antenna with good band-rejected function is proposed to demonstrate the superior features. The geometry of the proposed antenna is shown in Figure 11. The antenna is formed by the slot antenna described in Figure 1 and two sets of compound band-rejected structures. The first compound band-rejected structure consisted of an inverted C-shaped strip etched on the rectangular aperture and an inverted C-shaped slit near the top edge of the T-stub is employed to create the lower rejected band, while the other band-rejected structure formed by a C-shaped slit embedded in the feed-line and an inner C-shaped slit on the T-stub is employed to generate the upper rejected band. When the design parameters of the compound band-rejected structures are properly selected based on the rules described on the last section, two notched bands with excellent band-notched characteristics can be achieved.

It is necessary to control the notch bandwidths in practical application to obtain an effective band-notched UWB antenna. Therefore, the rejected bandwidths based on the widths and positions of the compound band-notched structures are studied. The specific

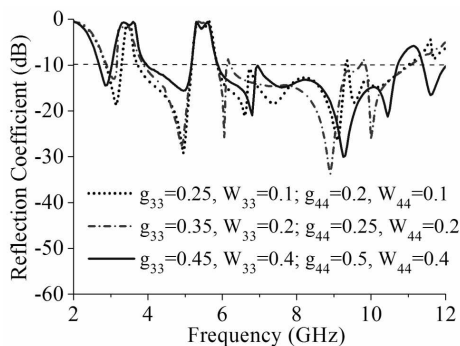


**Figure 12.** Effects of the parameters  $g_{33}$ ,  $W_{33}$ ,  $g_{44}$  and  $W_{44}$  for the first compound band-rejected structure on the band-notched function (units: mm);  $g_{11} = 6$  mm,  $W_{11} = 0.2$  mm,  $L_{11} = 1.9$  mm,  $L_{12} = 9.8$  mm,  $g_{22} = 1.5$  mm,  $W_{22} = 0.5$  mm,  $L_{33} = 11.6$  mm,  $L_{44} = 7.2$  mm. Short dot line:  $L_{22} = 4.5$  mm,  $L_{23} = 2.3$  mm,  $L_{34} = 6.5$  mm,  $L_{45} = 2.2$  mm; short dash dot line:  $L_{22} = 5.1$  mm,  $L_{23} = W_{22}$ ,  $L_{34} = 6.8$  mm,  $L_{45} = 2.3$  mm; solid line:  $L_{22} = 4.5$  mm,  $L_{23} = 2.1$ ,  $L_{34} = 6.5$  mm,  $L_{45} = 2.5$  mm.

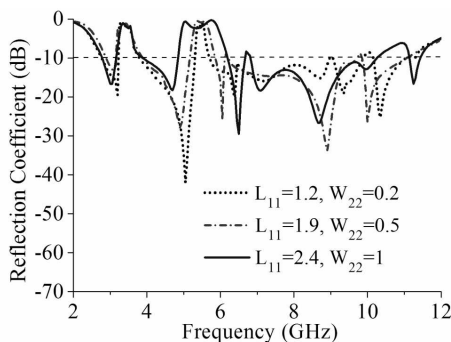


**Figure 13.** Effects of the parameters  $L_{11}$  and  $W_{22}$  for the second compound band-rejected structure on the band-notched function (units: mm);  $g_{11} = 6$  mm,  $W_{11} = 0.2$  mm,  $g_{22} = 1.5$  mm,  $g_{33} = 0.3$  mm,  $W_{33} = 0.2$  mm,  $L_{33} = 11.6$  mm,  $g_{44} = 0.2$  mm,  $W_{44} = 0.2$  mm,  $L_{44} = 7.5$  mm. short dot line:  $L_{12} = 10$  mm,  $L_{22} = 4.5$  mm,  $L_{23} = W_{22}$ ,  $L_{34} = 6.8$  mm,  $L_{45} = 2.6$  mm; short dash dot line:  $L_{12} = 9.6$  mm,  $L_{22} = 5.1$  mm,  $L_{23} = W_{22}$ ,  $L_{34} = 6.8$  mm,  $L_{45} = 2.5$  mm; solid line:  $L_{12} = 9.2$  mm,  $L_{22} = 5.5$  mm,  $L_{23} = 3$  mm,  $L_{34} = 7.2$  mm,  $L_{45} = 1.5$  mm.

frequencies around 3.5 GHz and 5.5 GHz for comparing the effects on the widths and positions of these parasitic slits and strip are set here. Figure 12 exhibits the effects of the parameters  $g_{33}$ ,  $W_{33}$ ,  $g_{44}$  and  $W_{44}$  of the first compound structure on the rejected bandwidth. The lower rejected bandwidth becomes wider as  $g_{33}$ ,  $W_{33}$ ,  $g_{44}$  and  $W_{44}$  increase, and the result is similar to that of Figure 9, while the upper notched band has small effects. Figure 13 shows the band-notched characteristics as function of the parameters  $L_{11}$  and  $W_{22}$  of the second band-notched structure. The upper rejected bandwidth is enhanced as  $L_{11}$  and  $W_{22}$  increase, and small effects on the lower band are observed.

Figures 14(a) and (b) show the current distributions at 3.5 GHz and 5.5 GHz on the proposed antenna, respectively, and large current distributions around the parasitic slits and strip are observed. In this case, destructive interference for the excited surface currents in the antenna will occur, which cause the antenna to be nonresponsive at those frequencies. At 3.5 GHz, large current distributed around the first set of compound band-rejected structure and small current flowed along the second set of band-rejected structure are seen, which indicates that the changed dimensions of the first compound band-notched structure has small effects on the upper rejected band. At 5.5 GHz, the current distributions mainly flow along the second compound band-rejected structure, while the currents around the first compound structure are small. In this way, the adjusted size for the second composite band-notched structure affects the lower band slightly.

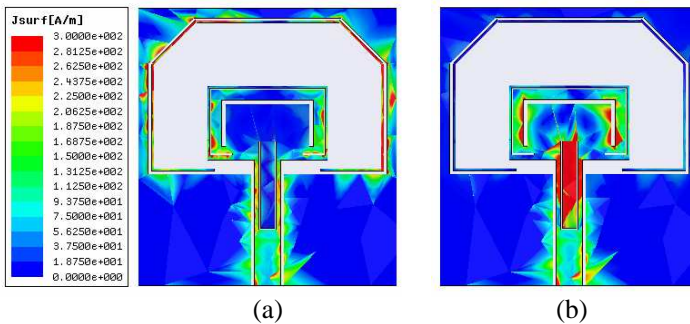


**Figure 14.** Current distribution of the proposed antenna at (a) 3.5 GHz, and (b) 5.5 GHz;  $g_{11} = 6$  mm,  $W_{11} = 0.2$  mm,  $L_{11} = 1.9$  mm,  $L_{12} = 9.8$  mm,  $g_{22} = 1.5$  mm,  $W_{22} = 0.5$  mm,  $L_{22} = 5.1$  mm,  $L_{23} = W_{22}$ ,  $g_{33} = 0.35$  mm,  $W_{33} = 0.2$  mm,  $L_{33} = 11.6$  mm,  $L_{34} = 6.8$  mm,  $g_{44} = 0.25$  mm,  $W_{44} = 0.2$  mm,  $L_{44} = 7.2$  mm,  $L_{45} = 2.3$  mm.

According to the above discussion, the overall design procedure for the proposed dual band-notched antenna can be summarized as follows. Firstly, design a T-stub fed rectangular aperture antenna with chamfered corners to cover the whole UWB operating band (3.1–10.6 GHz). Secondly, embed an inverted C-shaped strip near the top edge of the aperture and an inverted C-shaped slit near the top of the T-stub to create the lower rejected band, and then etch a C-shaped slit in the feed-line and an inner inverted C-shaped slit on the T-stub to generate the upper rejected band. Finally, optimize the sizes and locations of the slits and strip to get the required band-notched characteristics.

Finally, based on the design rules, an improved UWB antenna with dual band-rejected filtering properties in the WiMAX/WLAN bands is successfully designed. The design parameters are  $g_{11} = 6$  mm,  $W_{11} = 0.2$  mm,  $L_{11} = 1.9$  mm,  $L_{12} = 9.8$  mm,  $g_{22} = 1.5$  mm,  $W_{22} = 0.5$  mm,  $L_{22} = 5.1$  mm,  $L_{23} = W_{22}$ ,  $g_{33} = 0.35$  mm,  $W_{33} = 0.2$  mm,

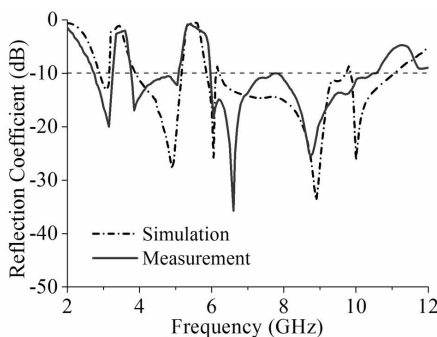
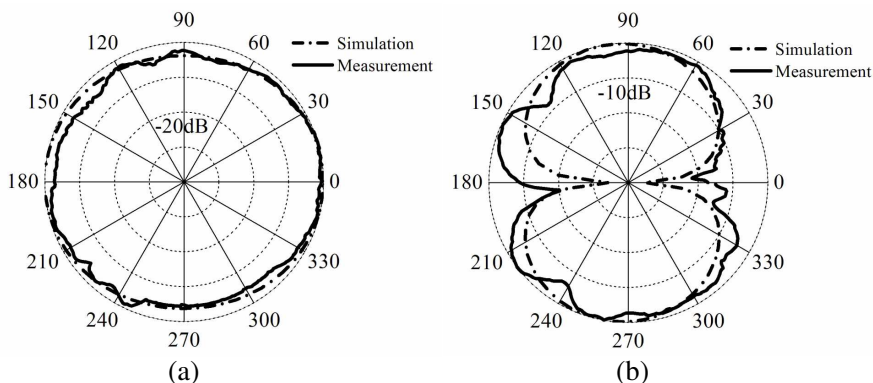
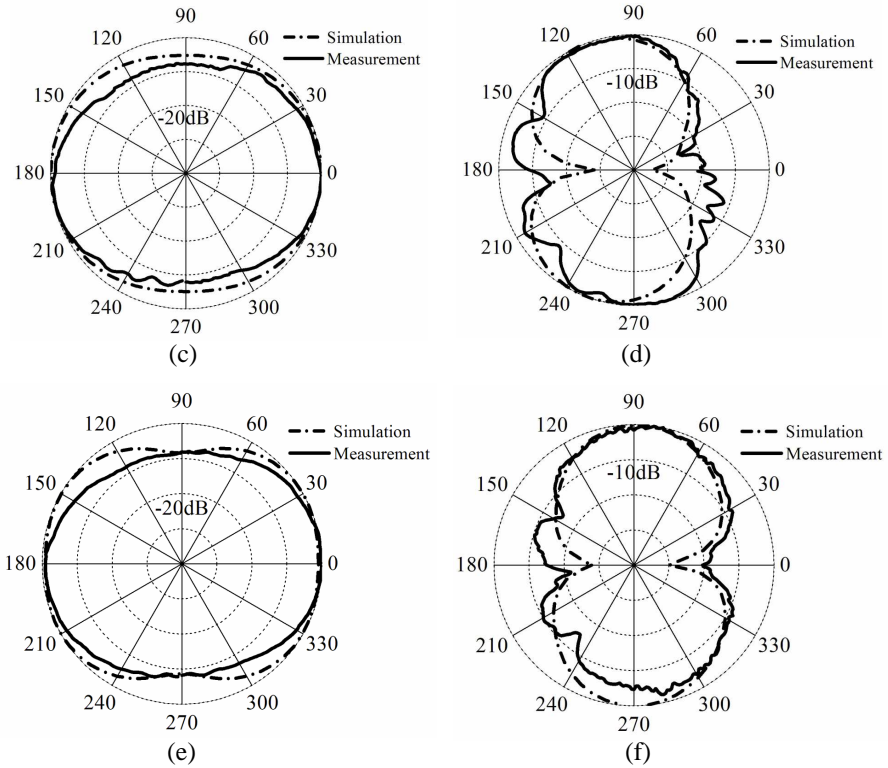


Figure 15. Measured reflection coefficient of the UWB antenna.





**Figure 16.** Radiation patterns of the proposed antenna. (a)  $H$ -plane ( $xy$ ) at 4.5 GHz. (b)  $E$ -plane ( $xz$ ) at 4.5 GHz. (c)  $H$ -plane ( $xy$ ) at 6.5 GHz. (d)  $E$ -plane ( $xz$ ) at 6.5 GHz. (e)  $H$ -plane ( $xy$ ) at 8 GHz. (f)  $E$ -plane ( $xz$ ) at 8 GHz.

$L_{33} = 11.6$  mm,  $L_{34} = 6.8$  mm,  $g_{44} = 0.25$  mm,  $W_{44} = 0.2$  mm,  $L_{44} = 7.2$  mm,  $L_{45} = 2.3$  mm. The reflection coefficient of the antenna is shown in Figure 15. According to the result, the antenna covers the band assigned for the UWB application. It is apparent that the proposed antenna can satisfy the UWB band (3.1–10.6 GHz) for  $S_{11} < 10$  dB, while rejecting the 3.2–3.8 GHz band for WiMAX and the 5.15–5.85 GHz band for WLAN.

The measured and simulated radiation patterns of the proposed antenna in the  $H$ -plane ( $xy$ -plane) and  $E$ -plane ( $xz$ -plane) for three different frequencies 4.5, 6.5 and 8 GHz are shown in Figure 16, and good agreement between the simulation and measurement are obtained. The patterns in the  $H$ -plane are quite omnidirectional as

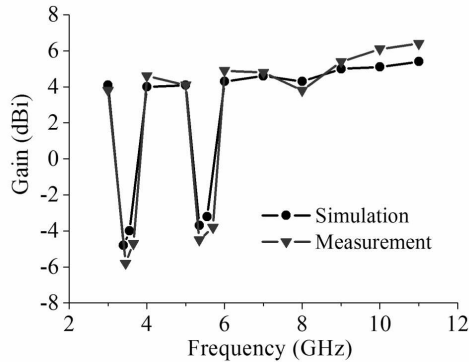


**Figure 17.** Gains of the proposed antenna.

expected. In the  $E$ -plane, the radiation patterns remain roughly a dumbbell shape like a small dipole leading to bidirectional patterns. For simplicity, the radiation patterns of antenna 1 to 5 are not depicted in this paper. To the best of authors' knowledge, the proposed band-notched structures including the single band-notched and dual band-notched ones have little influence on the radiation patterns of the UWB antenna. Figure 17 shows the measured and simulated gain of the proposed antenna. Sharp gain decreases occur in the vicinity of 3.5 and 5.5 GHz bands. However, for other frequencies outside the rejected bands, the antenna gain is nearly constant in the entire UWB band.

#### 4. CONCLUSION

An improved dual band-notched antenna with controllable notched bandwidths has been proposed. Compound band-rejected technique was provided to create much sharper, wider, and deeper notched bands within UWB frequency range compared with the previous published works. In addition, the frequency and width of the lower or upper rejected band can be independently controlled by adjusting the length, width and location of the corresponding compound band-rejected structure. Finally, a UWB slot antenna with two rejected bands at WiMAX/WLAN operating frequencies is successfully simulated, designed, and measured, showing good impedance matching, stable gain and near omnidirectional radiation patterns. Accordingly, the proposed antenna is expected to be a good candidate in various UWB systems.

## ACKNOWLEDGMENT

This work is supported by Guangdong key laboratory of clean energy technology (2008A060301002).

## REFERENCES

1. Zhang, X., Y.-Y. Xia, J. Chen, and W.-T. Li, "Compact microstrip-FED antenna for ultra-wideband applications," *Progress In Electromagnetics Research Letters*, Vol. 6, 11–16, 2009.
2. Dong, T. and Y. Chen, "Novel design of ultra-wideband printed double-sleeve monopole antenna," *Progress In Electromagnetics Research Letters*, Vol. 9, 165–173, 2009.
3. Chen, D. and C.-H. Cheng, "A novel compact ultra-wideband (UWB) wide slot antenna with via holes," *Progress In Electromagnetics Research*, Vol. 94, 343–349, 2009.
4. Danesfahani, R., L. Asadpor, and S. Soltani, "A small UWB CPW-fed monopole antenna with variable notched bandwidth," *Journal of Electromagnetic Waves and Applications*, Vol. 23, Nos. 8–9, 1067–1076, 2009.
5. Ren, W., J. Y. Deng, and K. S. Chen, "Compact PCB monopole antenna for UWB applications," *Journal of Electromagnetic Waves and Applications*, Vol. 21, No. 10, 1411–1420, 2007.
6. Siahcheshm, A., S. Sadat, C. H. Ghobadi, and J. Nourinia, "Design of a microstrip slot antenna filled by an isosceles triangle for UWB application," *Journal of Electromagnetic Waves and Applications*, Vol. 22, No. 1, 111–118, 2008.
7. Zhang, S., S. N. Khan, and S. He, "Modified rhombic monopole antenna for low loss frequency notched UWB applications," *Journal of Electromagnetic Waves and Applications*, Vol. 23, Nos. 2–3, 361–368, 2009.
8. Zhou, H.-J., Q.-Z. Liu, Y.-Z. Yin, and W. B. Wei, "Study of the band-notch function for swallow-tailed planar monopole antennas," *Progress In Electromagnetics Research*, Vol. 77, 55–65, 2007.
9. Naghshvarian-Jahromi, M., "Compact UWB bandnotch antenna with transmission-line-fed," *Progress In Electromagnetics Research B*, Vol. 3, 283–293, 2008.
10. Gopikrishna, M., D. D. Krishna, A. R. Chandran, and C. K. Aanadan, "Square monopole antenna for ultra wideband communication applications," *Journal of Electromagnetic Waves and Applications*, Vol. 21, No. 11, 1525–1537, 2007.

11. Fallahi, R., A. A. Kalteh, and M. G. Roozbahani, "A novel UWB elliptical slot antenna with band-notched characteristics," *Progress In Electromagnetics Research*, Vol. 82, 127–136, 2008.
12. Peng, L., C.-L. Ruan, Y.-L. Chen, and G.-M. Zhang, "A novel band-notched elliptical ring monopole antenna with a coplanar parasitic elliptical patch for UWB applications," *Journal of Electromagnetic Waves and Applications*, Vol. 22, No. 4, 517–528, 2008.
13. Zhang, L. N., S. S. Zhong, C. Z. Du, and J. H. Chen, "Compact UWB planar monopole antenna with band-notch function," *Microw. Opt. Technol. Lett.*, Vol. 51, No. 8, 1908–1911, 2009.
14. Zhang, Y., W. Hong, C. Yu, Z. Q. Kuai, Y. D. Don, and J. Y. Zhou, "Planar ultrawideband antennas with multiple notched bands based on etched slots on the patch and or split ring resonators on the feed line," *IEEE Trans. Antennas Propag.*, Vol. 56, No. 9, 3063–3068, 2008.
15. Sun, J.-Q., X.-M. Zhang, Y.-B. Yang, R. Guan, and L. Jin, "Dual band-notched ultra-wideband planar monopole antenna with M- and W-slots," *Progress In Electromagnetics Research Letters*, Vol. 19, 1–8, 2010.
16. Deng, J. Y., Y. Z. Yin, J. Ma, and Q. Z. Liu, "Compact ultra-wideband antenna with dual band-notched characteristic," *Journal of Electromagnetic Waves and Applications*, Vol. 23, No. 1, 109–116, 2009.